Global Change Biology

Global Change Biology (2017) **23**, 2396–2412, doi: 10.1111/gcb.13558

Plants, microorganisms, and soil temperatures contribute to a decrease in methane fluxes on a drained Arctic floodplain

MIN JUNG KWON[1], FELIX BEULIG[2,†], IULIA ILIE[1], MARCUS WILDNER[3,‡], KIRSTEN KÜSEL[2,4], LUTZ MERBOLD[5,§], MIGUEL D. MAHECHA[1,4], NIKITA ZIMOV[6], SERGEY A. ZIMOV[6], MARTIN HEIMANN[1,7], EDWARD A. G. SCHUUR[8], JOEL E. KOSTKA[9], OLAF KOLLE[1], INES HILKE[1] and MATHIAS GÖCKEDE[1]

[1]*Max Planck Institute for Biogeochemistry, Hans-Knöll-Str 10, 07745 Jena, Germany,* [2]*Aquatic Geomicrobiology, Institute of Ecology, Friedrich Schiller University Jena, Dornburgerstr 159, 07743 Jena, Germany,* [3]*Geoecology–Environmental Science: Micrometeorology and Atmospheric Chemistry, Faculty of Biology, Chemistry and Earth Science, University of Bayreuth, Universitätsstr 30, 95447 Bayreuth, Germany,* [4]*German Centre for Integrative Biodiversity Research (iDiv), Deutscher Platz 5d, 04103 Leipzig, Germany,* [5]*Department of Environmental Systems Science, Institute of Agricultural Sciences, ETH Zurich, Universitätstr 16, 8092 Zürich, Switzerland,* [6]*North-East Science Station, Pacific Institute for Geography, Far-Eastern Branch of Russian Academy of Science, PO Box 18, Cherskii, Republic of Sakha (Yakutia), Russia,* [7]*Division of Atmospheric Sciences, Department of Physics, PO Box 64, FI-00014 University of Helsinki, Helsinki, Finland,* [8]*Center for Ecosystem Science and Society, Department of Biological Sciences, Northern Arizona University, PO Box 5620, Flagstaff, AZ 86011, USA,* [9]*School of Biology, Georgia Institute of Technology, North Avenue, Atlanta, GA 30332, USA*

Abstract

As surface temperatures are expected to rise in the future, ice-rich permafrost may thaw, altering soil topography and hydrology and creating a mosaic of wet and dry soil surfaces in the Arctic. Arctic wetlands are large sources of CH_4, and investigating effects of soil hydrology on CH_4 fluxes is of great importance for predicting ecosystem feedback in response to climate change. In this study, we investigate how a decade-long drying manipulation on an Arctic floodplain influences CH_4-associated microorganisms, soil thermal regimes, and plant communities. Moreover, we examine how these drainage-induced changes may then modify CH_4 fluxes in the growing and nongrowing seasons. This study shows that drainage substantially lowered the abundance of methanogens along with methanotrophic bacteria, which may have reduced CH_4 cycling. Soil temperatures of the drained areas were lower in deep, anoxic soil layers (below 30 cm), but higher in oxic topsoil layers (0–15 cm) compared to the control wet areas. This pattern of soil temperatures may have reduced the rates of methanogenesis while elevating those of CH_4 oxidation, thereby decreasing net CH_4 fluxes. The abundance of *Eriophorum angustifolium*, an aerenchymatous plant species, diminished significantly in the drained areas. Due to this decrease, a higher fraction of CH_4 was alternatively emitted to the atmosphere by diffusion, possibly increasing the potential for CH_4 oxidation and leading to a decrease in net CH_4 fluxes compared to a control site. Drainage lowered CH_4 fluxes by a factor of 20 during the growing season, with postdrainage changes in microbial communities, soil temperatures, and plant communities also contributing to this reduction. In contrast, we observed CH_4 emissions increased by 10% in the drained areas during the nongrowing season, although this difference was insignificant given the small magnitudes of fluxes. This study showed that long-term drainage considerably reduced CH_4 fluxes through modified ecosystem properties.

Keywords: aerenchyma, closed dynamic chamber, fall methane fluxes, methanogens, Siberia

Received 1 August 2016; revised version received 31 October 2016 and accepted 1 November 2016

[†]Present address: Center for Geomicrobiology, Department of Bioscience, Aarhus University, Ny Munkegade 114 - 116, 8000 Aarhus C, Denmark

[‡]Present address: Leibniz Institute of Freshwater Ecology and Inland Fisheries, Müggelseedamm 310, 12587 Berlin, Germany

[§]Present address: International Livestock Research Institute, Mazingira Centre, PO Box 30709, 00100 Nairobi, Kenya

Correspondence: Min Jung Kwon, tel. +49 3641 576303, fax +49 3641 577300, e-mail: mkwon@bgc-jena.mpg.de

Introduction

Atmospheric temperatures in the Arctic have risen (Serreze *et al.*, 2000; Serreze & Barry, 2011), and this trend will likely continue in the near future (Collins *et al.*, 2013; Overland *et al.*, 2014). Warmer temperatures deepen permafrost thaw, and areas with abundant ice

lenses and wedges may subside as ice melts (Jorgenson *et al*., 2006; O'Donnell *et al*., 2011). In response to subsidence, surface water drains laterally to depressed areas, causing the soil topography and soil hydrology to become more heterogeneous, with a mosaic of wetter and drier soil surfaces. On an extended spatial and temporal scale, the number of thermokarst lakes can increase (Jorgenson *et al*., 2006) or decrease (Smith *et al*., 2005) from extensive thawing of permafrost, depending on local hydrological and topographical conditions (Morgenstern *et al*., 2013). Fluctuations in soil hydrology in the Arctic can also be aggravated or alleviated by strongly varying precipitation patterns. Overall, precipitation in the Arctic has increased over the last five decades (Kattsov & Walsh, 2000), and is forecast to increase further due to intensified hydrological cycles (Huntington, 2006; Kirtman *et al*., 2013; Bintanja & Selten, 2014). However, precipitation patterns are characterized by high spatiotemporal variability (Curtis *et al*., 1998; Stafford *et al*., 2000), potentially amplifying both wetter and drier soil conditions due to thawing permafrost.

Arctic ecosystems, primarily wetlands (Matthews & Fung, 1987; Aselmann & Crutzen, 1989), emit 25 ± 14 Tg CH_4 annually (McGuire *et al*., 2012); this represents approximately 10% of the global CH_4 emissions from natural wetlands (Ciais *et al*., 2013; Kirschke *et al*., 2013). As soil hydrology is expected to change, predicting the fate of the vast amount of organic carbon stored in Arctic permafrost soils (Hugelius *et al*., 2014; Schuur *et al*., 2015) – which corresponds to approximately 40% of global soil organic carbon within the top 3 m (Batjes, 1996; Jobbágy & Jackson, 2000) – is critical. In this study, we focus on how long-term drier conditions alter ecosystem properties, which then affect CH_4 fluxes. Our investigation into fluxes was carried out on a floodplain of the Yedoma region, which is characterized by ice-rich Pleistocene loess with abundant organic carbon (Zimov *et al*., 2006).

When water table falls, growing-season CH_4 fluxes generally become lower mainly due to more oxic conditions (van der Molen *et al*., 2007; Rhew *et al*., 2007; Merbold *et al*., 2009; Sturtevant *et al*., 2012), leading to shifts in microbial community structure, and most importantly a lower abundance of methanogens (Wagner *et al*., 2003; Høj *et al*., 2006; McCalley *et al*., 2014; Christiansen *et al*., 2015). Other factors, such as plant species composition (Morrissey & Livingston, 1992; King *et al*., 1998; Tsuyuzaki *et al*., 2001; Kutzbach *et al*., 2004; von Fischer *et al*., 2010; McEwing *et al*., 2015; Andresen *et al*., 2016), temperature (Nakano *et al*., 2000; Tveit *et al*., 2015), and thaw depth (TD; Kim, 2015), are also known to play important roles in CH_4 fluxes. The relative importance of the three main pathways of CH_4 transport to the atmosphere – ebullition, aerenchymatous plants, and diffusion – may also be altered, further modifying CH_4 fluxes.

Although previous observations in areas with an artificially lowered water table showed a consistent reduction in CH_4 fluxes during the growing season (Merbold *et al*., 2009; Sturtevant *et al*., 2012; Kim, 2015), no studies have investigated the long-term impact of drier conditions on CH_4 fluxes by taking altered ecosystem properties into account. Moreover, little is known about the CH_4 cycle during the nongrowing season in the Arctic. CH_4 fluxes during the nongrowing season can be more influenced by physical factors in comparison with the growing season. This is due to the fact that a limited availability of water and substrates in the frozen soil can hinder rates of soil microbial processes and frozen soil can inhibit gas exchange between the terrestrial ecosystem and the atmosphere. When soil freezes, waterlogged areas have shown both sporadic (Wille *et al*., 2008) and constantly high (Mastepanov *et al*., 2008, 2013) CH_4 fluxes in space and time, with the dominant plant species and water table leading to variations in the magnitude of fluxes (Whalen & Reeburgh, 1992). However, higher CH_4 fluxes have also been observed in dry tundra ecosystems than in wet ones (Zona *et al*., 2015). Due to the limited number of studies, it is as of yet unclear how water table variability affects CH_4 fluxes during the nongrowing season in the Arctic.

In this study, we present (1) how decade-long drainage affects CH_4-associated microorganisms, soil temperature (T_{soil}), and plant community structure and (2) how these modifications contribute to CH_4 fluxes during the growing season and (3) nongrowing season. In addition, we aim to identify the biotic and abiotic controlling factors of CH_4 fluxes. This is the first manipulation study to show the effects of decade-long drainage on CH_4 fluxes in the Arctic.

Materials and methods

Site description

The study site is located on a floodplain of the Kolyma River near Chersky, Northeastern Siberia. For the period of 1960–2009, monthly average temperatures ranged between −33 °C and +12 °C (Berkeley Earth project, berkeleyearth.org, Station ID: 169921). For the period of 1950–1999, average annual precipitation at Chersky weather station was 197 mm (World Meteorological Organization, WMO). Water level of the site increases up to 50 cm above the soil surface between May and early June due to snow melt at the site and flooding from the nearby river basin and decreases gradually from mid-June to mid-July. Tussock-forming sedges, *Carex appendiculata*, and cotton sedges, *Eriophorum angustifolium*, are the dominant plant species. An organic peat layer (15–25 cm) lies on top of alluvial materials, which are composed of silty clay. Some

organic peat materials can be found in alluvial layers due to cryoturbation.

In 2013, two areas were selected to investigate the effects of drainage: The first area had been drained by a ditch since 2004 (drained; 68°36′47″ N, 161°20′29″ E; Merbold *et al*., 2009), while the control area has not been affected by any manipulation of water level (control; 68°37′00″ N, 161°20′59″ E). The two areas are located approximately 600 m away from each other. Within each of these two areas, a transect with 10 plots was established (henceforth referred to as the drained and the control transects, respectively), in which CH_4 fluxes and ecosystem properties were measured. Plots were selected using a stratified systematic sampling method: 10 positions were preselected at 25-m intervals along the transect, and then, final plots were purposively chosen to reflect the representative plant species in the surrounding areas. Due to variability in topography and the resulting heterogeneous microsite characteristics, both the drained and the control transects included water-saturated and unsaturated plots. We used mean water levels to group 10 plots within each transect into wet and dry categories: The plots were labeled as 'wet' when the average water table over the growing season was higher than −10 cm, otherwise 'dry'. This scheme yielded four groups by drainage manipulation (i.e., transect) and water table category (Fig. 1). Additionally, one plot was selected from each of the four groups as the core plot. Throughout this study, all results are presented using these group designations, with the same color palette as used in Fig. 1.

We conducted three field campaigns: (1) summer 2013 (20 July to 10 August; representing the mid-growing season), (2) fall 2013 (1 November to 30 November; representing the nongrowing fall season), and (3) summer 2014 (15 June to 20 August; representing the early- and mid-growing season). The growing season campaigns of both years included the peak of the growing season as identified by the Normalized Difference Vegetation Index (NDVI) maximum: July 29, 2013, and August 4, 2014, respectively (Kittler *et al*., 2016). In 2013, all 20 plots were visited equally, on average two times per week during a 3- and 4-week observation period in summer and fall, respectively; this regular sampling gave good coverage of spatial variation in fluxes and environmental variables during the middle of the growing and nongrowing seasons. A different method was chosen for 2014: In 2014, one plot from each of the four categories listed above was selected as a core plot, and was visited more frequently (on average three times a week) than the rest of the plots for 10 weeks of the observation period; this allowed temporal variation to be captured over a longer period of the growing season (Fig. 1).

Water table, TD, and T_{soil}

Water table was measured in parallel with flux measurements within permanently installed perforated polyvinyl chloride pipes (ø 25 mm) at each plot. Water table was assessed relative to the soil surface, with values >0 cm denoting water standing above the soil surface. TD was measured at the same time as water table by pushing a measuring pole into the ground. T_{soil} was measured at 5, 15, 25, and 35 cm depths (Th3-s, UMS, Germany) in all even-numbered plots including core plots. As T_{soil} and TD increase over the growing season, to minimize seasonality in data, the 2014 growing season was divided into four 15-day subseasons, beginning from June 15, 2014: (1) Subseason 1 (15–30 June), (2) Subseason 2 (1–15 July), (3) Subseason 3 (16–31 July), and (4) Subseason 4 (1–20 August). Data from the 2013 growing season were not divided into subseasons because the variations within the 3 weeks of the observation period were not distinct. The period of the 2013 growing season was comparable to Subseason 4 of the 2014 growing season, with both periods containing the highest NDVI.

CH_4 fluxes and pathways

We measured CH_4 fluxes using a non-steady-state flow-through (i.e., closed dynamic) chamber (60 cm on each side, made in-house of transparent Plexiglas). CH_4 concentrations ($[CH_4]$) were measured using an Ultra-Portable Greenhouse Gas Analyzer (UGGA; Los Gatos Research, San Jose, CA, USA), and all data were acquired using a logger at 1-Hz temporal resolution (CR1000; Campbell Scientific, Logan, UT, USA). The time for measuring changes in $[CH_4]$ was restricted to a maximum of 2 min to minimize biases related to saturation and pressure effects. Ice packs were placed inside the chamber before measuring fluxes to prevent the temperature from rising more than 1 °C per min, in the event of strong incoming radiation, and three small fans were installed in one corner inside the chamber headspace to ensure continuous air mixing. Air temperature (T_a), relative air humidity, air pressure (P_a), and photosynthetically active radiation (PAR) were measured inside the chamber in parallel with $[CH_4]$. To calculate CH_4 fluxes, median values of the linear $[CH_4]$ slopes were computed for multiple time windows, which were randomly assigned through a bootstrapping approach, and fluxes were calculated taking T_a, P_a, and the volume and the area of chamber into account (Rochette & Hutchinson, 2005). As diurnal variations were found to be negligible during the growing and nongrowing seasons, fluxes were interpolated to daily mean flux rates (Fig. S1). Finally, daily CH_4 fluxes of each plot were linearly interpolated to acquire the growing-season CH_4 fluxes, assuming that not-measured CH_4 fluxes between measurement days fell in the range of CH_4 fluxes measured. Nongrowing-season CH_4 fluxes were measured on top of the snowpack (thickness of 40 cm on average across the two transects at the end of November), and flux rates were not linearly interpolated due to the sporadic occurrence of high fluxes.

To estimate the extent of CH_4 transport through *E. angustifolium*, an aerenchymatous plant, we placed a single plant into a cylindrical dark chamber (ø 10 cm × 50 cm height) and sealed the base with a gas-tight cap that enclosed the plant. Diverse sizes of plants (stem diameters 0.3–1.5 cm, green leaf lengths 21–97 cm) were selected near the chamber collars. Because fans were not installed in the plant chamber, we drew gas samples with forked tubing at three different heights of the chamber to get representative flux rates, and recorded $[CH_4]$ for 2 min using an UGGA at 1-Hz time resolution. To calculate the fraction of the amount of CH_4 transported

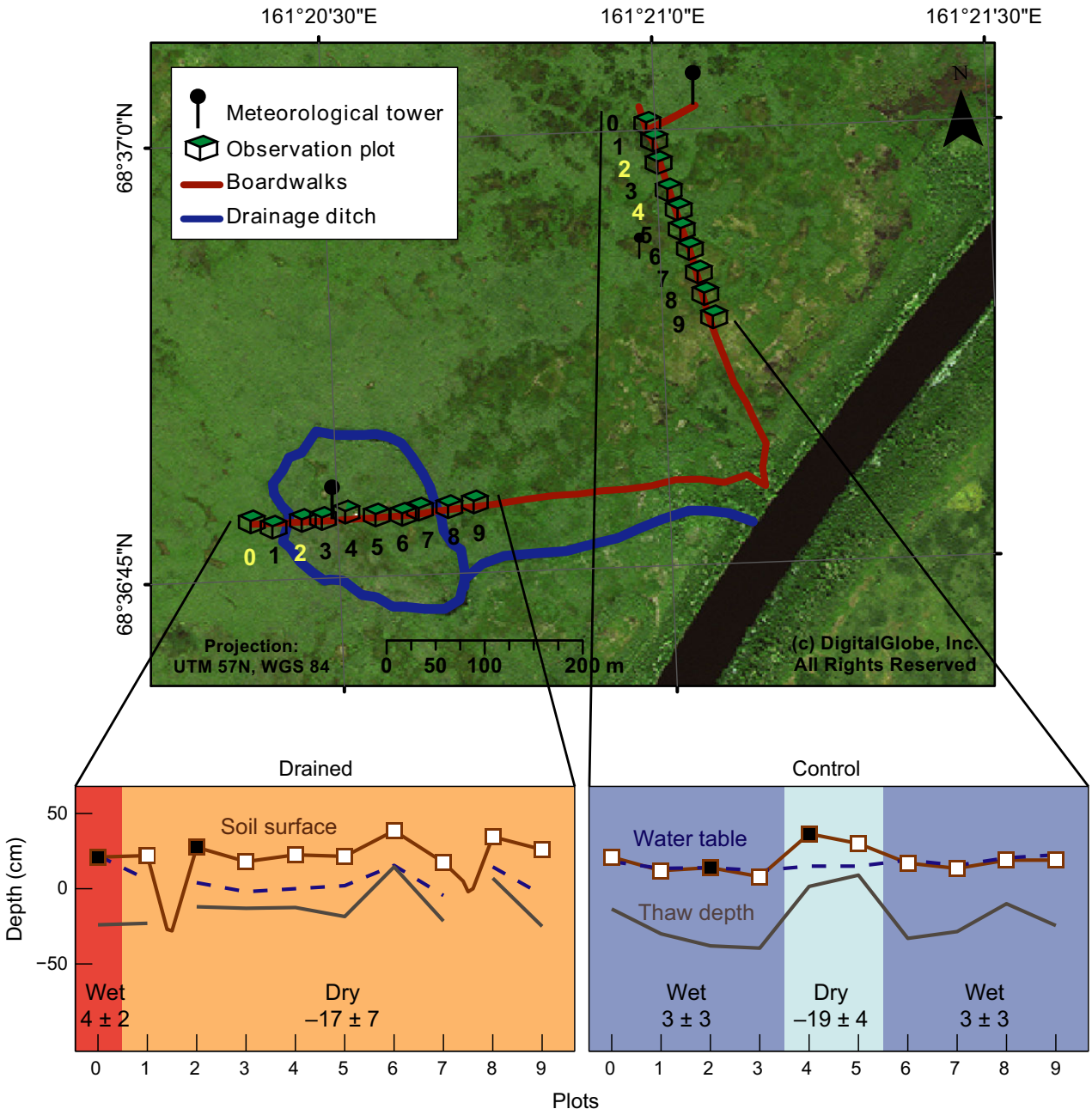

Fig. 1 Aerial map of the study site and soil hydrology and thawing properties across transects. The transect in the bottom left of the map is the drained transect, and the transect on the top right of the map is the control transect. Soil surface, water table, and thaw depth of each plot are described in parallel. Twenty plots were categorized into four groups by drainage manipulation (i.e., transect; drained or control) and water table category (wet or dry): drained_wet (marginally influenced by drainage; red), drained_dry (strongly influenced by drainage; salmon), control_wet (naturally inundated; blue), and control_dry (naturally dry due to higher soil topography; light blue). The core plots from each group are indicated with yellow numbers in the map and black squares in the figure. As one example of spatial variability, water table and thaw depth lines are drawn based on observations made on August 10, 2013. The average water table of each group (cm, mean ± SD) was calculated excluding June, when water table was influenced by spring snow melt and flooding. [Colour figure can be viewed at wileyonlinelibrary.com].

through *E. angustifolium*, the three following steps were applied: (1) Correlation analyses were carried out between the green leaf lengths and the amounts of CH_4 transported by a single plant, yielding a linear function that estimates flux rates based on plant height, (2) the average green leaf length of *E. angustifolium* inside the chamber collars was measured, and the expected amount of CH_4 transported by a single plant (mean and standard deviation) was calculated using the

functions derived from (1); and (3) the number of plants found inside the chamber collars was multiplied by the mean flux per plant from (2) to yield the total plant-mediated flux within the chamber area. The uncertainty ranges of this estimate were computed by modifying the green leaf lengths by 10 cm and the number of plants by 5. In Step (1), green leaf length was chosen because it showed the strongest positive correlations with the amount of CH_4 emitted through *E. angustifolium* compared to other plant traits, such as stem diameter or number of green leaves.

Ebullition events were detected by examining the trajectories of [CH_4] plotted over time during 2-min flux measurements. When [CH_4] increased linearly within 2 min, the CH_4 transport was regarded as a mixture of diffusion and plant-mediated transport (Fig. S2a). However, when an abrupt increase in [CH_4] was detected between two linear slopes, this event was defined as ebullition (Fig. S2b). For all 2-min [CH_4] measurements over the growing season, the proportion of ebullition events to the total CH_4 fluxes – frequency and the amount of carbon emitted through ebullition – was calculated using the equations below:

$$\text{Frequency} = \frac{\text{the number of ebullition events}}{\text{the total number of flux measurement}}, \quad (1)$$

$$\text{Ebullition} = \frac{\text{the amount of } CH_4 \text{ through ebullition}}{\text{the total amount of } CH_4 \text{ flux}} \times \text{frequency} \times 100\,(\%). \quad (2)$$

This estimation was based on the assumption that the frequency of ebullition within 2-min measurements represents the natural conditions well and that both diurnal variation in frequency and the size of ebullition events are negligible. Ebullition events that occurred within 30 s after the chamber head was placed on the collar – it took about 20 s for the gas from the chamber to travel to the analyzer – were evaluated separately because they may have been triggered by physical disturbances.

Soil sampling

Five soil cores (ø 7.6 cm) were taken from the active layer (~30 cm) of each transect in July 2013. Each core was divided into an organic peat layer and an alluvial soil layer, and then, each layer was further divided in 7.5-cm increments, leading to three to five increments per core. Soils were transferred directly after sampling to the laboratory and stored at 4 °C until analysis. Subsamples of soils were dried at 105 °C for 24 h to derive gravimetric soil moisture (%). Total carbon (%) was estimated after drying peat soils at 70 °C and alluvial soils at 40 °C (varioEL; Elementar, Hanau, Germany). Bulk density of soils (g cm^{-3}) was estimated at the core plots (drained, $N = 3$; control, $N = 1$).

DNA extraction

Soil cores from the core plots were selected for microbial analysis. Subsamples of soils were conserved in soil preservation solution (Life Guard Soil Preservation Solution; Mo Bio Laboratories, Carlsbad, CA, USA) and kept frozen at −20 °C until extraction. Each sample was split into three to create triplicates. Total genomic DNA was extracted through the following sequence: (1) 0.5 g of soil was mixed with 0.5 g of zirconia beads (ø 0.1 mm), 0.75 mL sodium phosphate buffer solution (112.9 mM Na_2HPO_4, 7.1 mM NaH_2PO_4), and 0.25 mL sodium dodecyl sulfate (SDS) buffer solution (500 mM Tris-HCl, 100 mM NaCl, 10% w/v SDS, pH 8.0). (2) The mixture was lysed for 45 s at a speed of 6.5 m/s (FastPrep-24; MP Biomedicals, Santa Ana, CA, USA). (3) After centrifugation at 18,000× g for 5 min, supernatant was extracted using equal volumes of first phenol:chloroform: isoamylalcohol (25:24:1 v:v:v; Sigma-Aldrich, St. Louis, MO, USA) and then chloroform:isoamylalcohol (24:1 v:v; Sigma-Aldrich, USA). (4) Nucleic acids were precipitated from 0.5 mL of extract using 1 mL poly (ethylene glycol) 8,000 (Sigma-Aldrich, USA), incubating at 4 °C overnight and centrifuging at 19,000× g for 30 min. (5) The precipitate from Step (4) was washed with 0.4 mL ice-cold ethanol solution (70% v/v) and dissolved in 500 μL TE buffer (10 mM Tris, 1 mM EDTA, pH 8.0). (6) The extract was filtered to remove co-extracted organic contaminants (OneStep™ PCR Inhibitor Removal Kit; Zymo Research, Irvine, CA, USA) and samples that remained contaminated (detected using the ND-1000 Spectrophotometer; Thermo Fisher Scientific, Waltham, MA, USA) were purified again by repeating the steps (3) to (6).

Illumina sequencing and data processing

The diversity and composition of prokaryotic communities were determined by applying a high-throughput sequencing-based protocol that targets PCR-generated amplicons from V4 variable regions of the 16S rRNA gene using the bacterial primer set 515F (5′-GTGCCAGCMGCCGCGGTAA-3′) and 806R (5′-GGACTACHVGGGTWTCTAAT-3′) (Caporaso *et al*., 2011). Amplicons were barcoded, and sequencing was conducted on an Illumina MiSeq platform at the Research Resources Center (RRC) of the University of Illinois at Chicago, following standard protocols (Caporaso *et al*., 2012; Gilbert *et al*., 2014; http://www.earthmicrobiome.org/emp-standard-protocols/16s/). The generated sequence data are available from the European Nucleotide Archive (ENA, Study accession number: PRJEB14835). MiSeq paired-end raw reads were demultiplexed and then processed using the program MOTHUR version 1.33 (Schloss *et al*., 2009), using the following criteria: (1) the 300-bp reads were truncated at any site that obtained an average quality score of <20 over a 50-bp sliding window, and any truncated reads <50 bp were discarded, (2) reads with any mismatch in barcode, more than two nucleotide mismatch in primer, or containing ambiguous characters were removed, (3) overlapping sequences <10 bp or with a mismatch ratio of more than 0.2 within the overlap region were eliminated, (4) sequences were trimmed to a common length of 250 bp, and (5) chimeric sequences were filtered out by UCHIME (Edgar *et al*., 2011). (6) To ensure a better comparison of samples that had different numbers of sequence reads, read numbers of each sample were normalized to the size of the smallest data set (14,670). (7) Operational taxonomic

units (OTUs) were classified as those with at least a 97% sequence similarity (SILVA database). Sequencing coverage was 92% on average with a minimum 84%. To investigate whether drainage affects the community structures of CH_4-associated microorganisms, the fractions and the compositions of methanogens and methanotrophs were investigated.

Quantitative PCR

The abundance of bacterial and archaeal 16S rRNA genes in DNA extracts was quantified using quantitative PCR (qPCR) on a Mx3000P instrument (Agilent Technologies, Santa Clara, CA, USA). The primer combinations A-806F and A-958R (V5 region; DeLong, 1992; Takai & Horikoshi, 2000) and B-28F and B-338R (V1–V2 region; Daims *et al*., 1999; Loy *et al*., 2002) were used, as described in previous studies (Herrmann *et al*., 2012).

Plant community structure

To investigate the impact of 10 years of drainage on the abundance of aerenchymatous plant species, all living vegetation inside 1 × 1 m^2 quadrats was harvested in 2013 ($N = 4$ quadrats per transect). This harvest took place along the same transect used in 2003, which predated the installation of a drainage ditch in 2004 (Corradi *et al*., 2005). Plants were sorted by species and dried at 40 °C to derive the dry weight. Relative abundance of each species (%) was calculated based on the dry biomass for 2003 and 2013 data. We also applied the nondestructive point-intercept method within chamber collars, dividing each 60 × 60 cm^2 quadrat into 10 × 10 cm^2 subgrids to directly correlate CH_4 fluxes with aerenchymatous plant cover. We recorded the plant species that a laser pointer hit when pointed downward at each subgrid intersection, and calculated the percentage that each species covered in each plot.

Statistical analysis

A two-way analysis of variance (ANOVA) was performed to investigate any differences in total carbon by transect and water table category. Bulk density was compared between wet and dry plots of the drained transect using an independent *t*-test. Two-way ANOVA was performed to determine whether the fractions of methanogens and methanotrophs varied by transect and water table category. Two-way permutational multivariate ANOVA (PERMANOVA) was carried out with the communities of methanogens and methanotrophs as the dependent variables to determine whether microbial community structures differed with transect and water table category. Regression analyses were performed for each transect with water table as the independent variables and T_{soil} at 5 cm, T_{soil} at 35 cm, and TD as the dependent variables, to determine whether T_{soil} and TD were affected by water table. Regression analyses were carried out for each transect to test dependencies, between CH_4 fluxes of the dry plots and T_{soil} at 5 cm, between CH_4 fluxes of the wet plots and T_{soil} at 35 cm, and between CH_4 fluxes and *E. angustifolium* cover. The abundance of *E. angustifolium* (estimated by destructive sampling) among the four groups from 2014, as well as the samples from 2003, was also compared using one-way ANOVA. If abundance differed significantly by group, Tukey's *post hoc* test was performed. All statistical analyses were performed using R (R Development Core Team 2013).

To compare the major environmental drivers for the growing- and the nongrowing-season CH_4 fluxes, we used a machine learning method that yields a symbolic regression. This method is a regression approach, whereby a variety of transformations and their multiplicative and additive interactions are tested. Methods of this kind are deployed to derive complex models in a purely data-driven way, which allows for data interpretation beyond linear statistics. Here, we used gene expression programming (GEP; Ferreira, 2001), combined with a covariance matrix adaptation evolution strategy (CMAES; Hansen *et al*., 2003) to identify optimal parameterizations of the identified models. In the following sections, we refer to this approach as CMAGEP (I. Ilie, P. Dittrich, M. Jung, N. Carvalhais & M. Mahecha, unpublished data). We applied the CMAGEP method to each transect as such: Candidate driving variables included in this analysis were the absolute values and temporal derivatives of continuously measured T_a, P_a, and PAR, as well as T_{soil} at 5–35 cm. In the array of candidate drivers for the CMAGEP-derived models, we also included the abundance of *E. angustifolium*, *C. appendiculata*, and *Potentilla palustris*, as well as water table and TD during the growing season. The settings used for each CMAGEP run are described in Table S1. For each transect, we generate 100 subsets of randomly selected data points. In each subset, 70% of the total number of data points are used for training 100 models. The rest of the data points are used to compute the validation fit of all models, with the model with the best fit at validation finally selected. Model evaluation and selection took into account the Akaike information criterion (AIC) values computed between the observed and modeled flux rates for all 100 data subsets. To ensure interpretability, the root-mean-square error (RMSE) and model bias error (MBE) were also computed across the entire dataset.

Results

Drainage effects on soils

Total soil carbon content was higher in the drained transect compared to the control transect in the organic soil layers (two-way ANOVA; drainage, $F = 25.40$, $P < 0.001$; water, $F = 0.56$, $P = 0.46$; drainage × water, $F = 1.83$, $P = 0.18$) and in the mineral soil layers (two-way ANOVA; drainage, $F = 11.69$, $P < 0.01$; water, $F = 12.24$, $P < 0.01$; drainage × water, $F = 7.46$, $P < 0.05$). Bulk density of organic layers in the dry plot was 55% higher than in the wet plot in the drained transect (*t*-test; $P = 0.01$, $t = -2.74$, df = 23.7). A similar pattern was observed for the control transect, showing

approximately 20% higher bulk density in the dry plot than in the wet plot.

Growing-season CH_4 fluxes and pathways

CH_4 fluxes were significantly influenced by water table: control_wet plots showed the highest CH_4 fluxes, and drained_wet plot the second highest, while dry plots showed considerably lower flux rates (Table 1, Fig. 2). Some of the dry plots showed negative net CH_4 exchange, suggesting that oxidation rates exceeded production rates (Table 1, Fig. 2). In 2014, the CH_4 flux rates were higher in the wet plots due to warmer temperatures and lower in the dry plots due to drier conditions compared to those in 2013 (Table 1). Fluxes of control_wet were about three times higher than those of drained_wet plot in both years despite similar water table (Table 1, Fig. 2). Weighting the average daily fluxes with the number of wet and dry plots of each transect resulted in approximately 19 and 28 times lower CH_4 emission rates compared to the control transect in 2013 and 2014, respectively (Table 1).

Table 1 Daily growing-season CH_4 flux rates (mean ± SD). 2013 data cover 18 days (24 July to 10 August) and 2014 data cover 62 days (20 June to 20 August). Values in parentheses for 2014 are mean daily flux rates covering the same observation period as in 2013. Each group of data from 2013 consists of multiple plots, while data from 2014 consist of the core plots only; the standard deviation values for 2013 therefore reflect both spatial and temporal variation, while those from 2014 reflect temporal variation only

	Daily CH_4 flux (mg CH_4 m^{-2} day^{-1})	
	2013	2014
Drained_wet	77 ± 13	105 ± 77 (169 ± 45)
Drained_dry	4 ± 14	−1 ± 2 (−2 ± 2)
Control_wet	267 ± 141	332 ± 168 (457 ± 98)
Control_dry	−2 ± 1	−3 ± 1 (−4 ± 1)

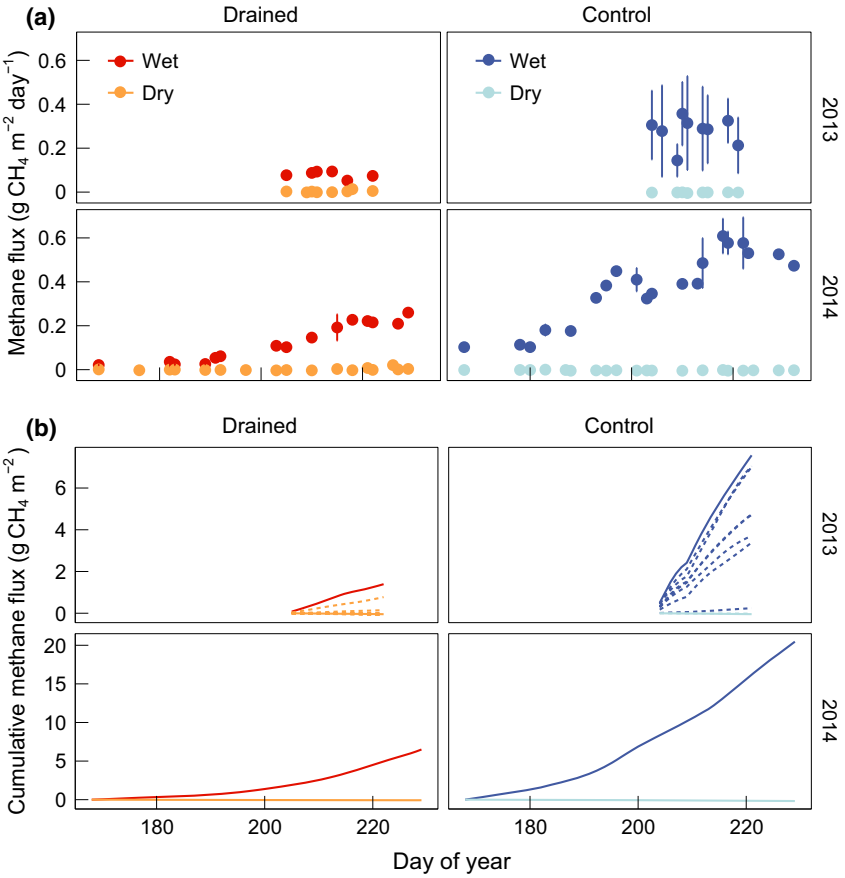

Fig. 2 CH_4 fluxes during the growing season of 2013 and 2014. (a) Points represent average daily CH_4 fluxes of each group (2013) or plot (2014), and error bars represent standard deviations from multiple plots (2013) or multiple measurements from a single plot (2014). (b) Cumulative CH_4 fluxes are based on linear interpolation by plot. Data covered 18 days (24 July to 10 August) in 2013 and 62 days (20 June to 20 August) in 2014. Solid lines in 2013 indicate fluxes at core plots that correspond to lines in 2014. Note that 2013 and 2014 have different scales. [Colour figure can be viewed at wileyonlinelibrary.com].

Table 2 Contribution of plant-mediated CH_4 transport and ebullition to total CH_4 fluxes. The percentage was calculated using the data acquired from July 23 to August 20, 2014. For plant-mediated transport, sensitivity of the estimate to changes in the green leaf length by 10 cm and to changes in the number of plants by five is presented. For ebullition, numbers in parentheses indicate ebullition events that occurred within 30 s after the chamber was placed on the collar, which may have resulted from physical disturbance

	Plant-mediated transport (%)	Sensitivity (%)	Ebullition (%)
Drained_wet	5 ± 1	±4	0 (+1)
Drained_dry	76 ± 303*	±679	0
Control_wet	25 ± 8	±19	2 (+2)
Control_dry	0†		0

*Higher than 100% values indicate that the amount of plant-mediated CH_4 transport was higher than the total CH_4 fluxes and that the difference therefore came from CH_4 oxidation.
†No *Eriophorum angustifolium* exists.

The contribution of plant-mediated transport through aerenchyma to the total CH_4 flux varied among the four categories: control_wet plots showed the highest contribution (25%), while the contribution in drained_wet plot was only 5% (Table 2). Control_dry plots did not transport CH_4 through aerenchyma because they did not have *E. angustifolium* (Table 2). Drained_dry plots showed a very high proportion (76%) of aerenchyma transport to total CH_4 fluxes, but the absolute values of total CH_4 fluxes were close to zero (Table 1, 2). CH_4 transport continued after plants were clipped right above the water table (data not shown), suggesting that plant-mediated CH_4 transport was not through active transport, but was diffusive in nature.

Overall, the contributions of ebullition to CH_4 flux rates were low. Control_wet plots emitted an average of 2% of CH_4 through ebullition, while no ebullition events were observed in any other plots (Table 2). When ebullition events that might have been due to disturbance are included, ebullition contributions increase to 4% in control_wet plots and to 1% in drained_wet plot (Table 2). The dry plots did not show any ebullition events in either case (Table 2).

Nongrowing-season CH_4 fluxes

CH_4 fluxes in the nongrowing season were generally lower compared to those in the growing season. However, some plots, especially drained_wet plots, showed sporadically high flux rates, which were comparable to those of the growing season (Figs 2 and 3). Very high CH_4 fluxes in the nongrowing season were partly induced by the higher *E. angustifolium* cover when P_a was decreasing (Fig. 3). When the observed CH_4 fluxes were averaged over the 4 weeks of the observation period, the drained transect emitted 11 mg CH_4 m^{-2} day^{-1}, while the control transect emitted 10 mg CH_4 m^{-2} day^{-1}.

Biotic and abiotic factors influencing CH_4 flux rates

A gene expression programming method revealed that the growing-season CH_4 flux rates were positively influenced by T_{soil} at deep layers and *E. angustifolium* cover as well as negatively by P_a and the *C. appendiculata* cover (drained: Eqn 3; control, Eqn 4). In the nongrowing season, although the structures of the equations differed from those of the growing season, similar parameters influenced CH_4 flux rates (drained, Eqn 5; control, Eqn 6).

Growing season, drained

$$\mathrm{CH_4\ fluxes}\left(\mathrm{mg\,CH_4\,m^{-2}\,s^{-1}}\right) = \frac{0.091 \times \mathrm{Tsoil\ at\ 35\ cm\ (^{\circ}C)}}{0.15 \times \mathrm{Pa\ (hPa)} + 4.3 \times \mathrm{Carex\ (\%)}}. \quad (3)$$

Model evaluation: 0.88, $R^2 = 0.90$, $P < 0.001$, RMSE = 0.001, MBE = −0.00007.

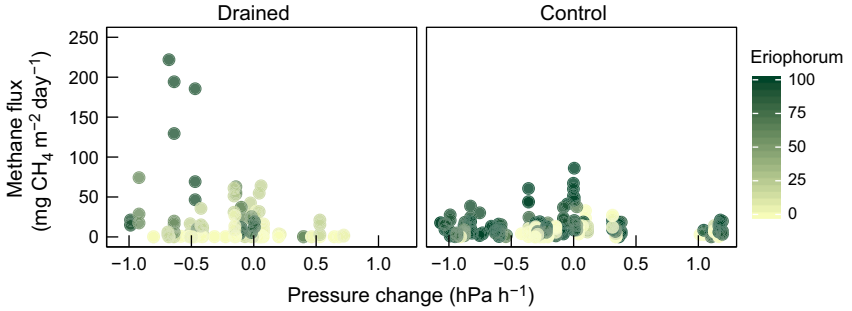

Fig. 3 Nongrowing-season CH_4 fluxes against changes in P_a. Data are from November 2013, and colors indicate the *Eriophorum angustifolium* cover. Changes in P_a refer to changes within 6 h before individual flux was measured. [Colour figure can be viewed at wileyonlinelibrary.com].

Growing-season, control

$$\mathrm{CH_4\ fluxes}\left(\mathrm{mg\,CH_4\,m^{-2}\,s^{-1}}\right) = \frac{0.056 \times \mathrm{Eriophorum}\,(\%)}{\mathrm{Pa\,(hPa)}}. \quad (4)$$

Model evaluation: 0.69, $R^2 = 0.70$, $P < 0.001$, RMSE = 0.007, MBE = −0.00007.

Nongrowing season, drained

$$\mathrm{CH_4\ fluxes}\left(\mathrm{mg\,CH_4\,m^{-2}\,s^{-1}}\right) = 30.0 \times \mathrm{Eriophorum}\,(\%) \times e^{1.302 \times \mathrm{Ta}\,(^{\circ}\mathrm{C})}. \quad (5)$$

Model evaluation: 0.11, $R^2 = 0.43$, $P < 0.001$, RMSE = 0.0004, MBE = −0.00003.

Nongrowing season, control

$$\mathrm{CH_4\ fluxes}\left(\mathrm{mg\,CH_4\,m^{-2}\,s^{-1}}\right) = \frac{0.093}{\mathrm{Pa\,(hPa)}}. \quad (6)$$

Model evaluation: 0.00, $R^2 = 0.08$, $P < 0.001$, RMSE = 0.0005, MBE = −0.00003.

CH_4-associated microorganisms and their effects on growing-season CH_4 fluxes

High CH_4 fluxes coincided with higher fractions of methanogens and methanotrophs (Fig. 4). The fraction of methanogens was highest in control_wet and lowest in control_dry plots (Fig. 4b). The two upper soil layers showed significant differences between the four groups in both the relative abundance (two-way ANOVA; drainage, $F = 4.67$, $P < 0.05$; water, $F = 6.50$, $P < 0.05$; drainage × water, $F = 6.31$, $P < 0.05$) and in community composition (two-way PERMANOVA; drainage, $F = 9.41$, $P < 0.001$; water, $F = 6.37$, $P < 0.001$; drainage × water, $F = 8.80$, $P < 0.001$):

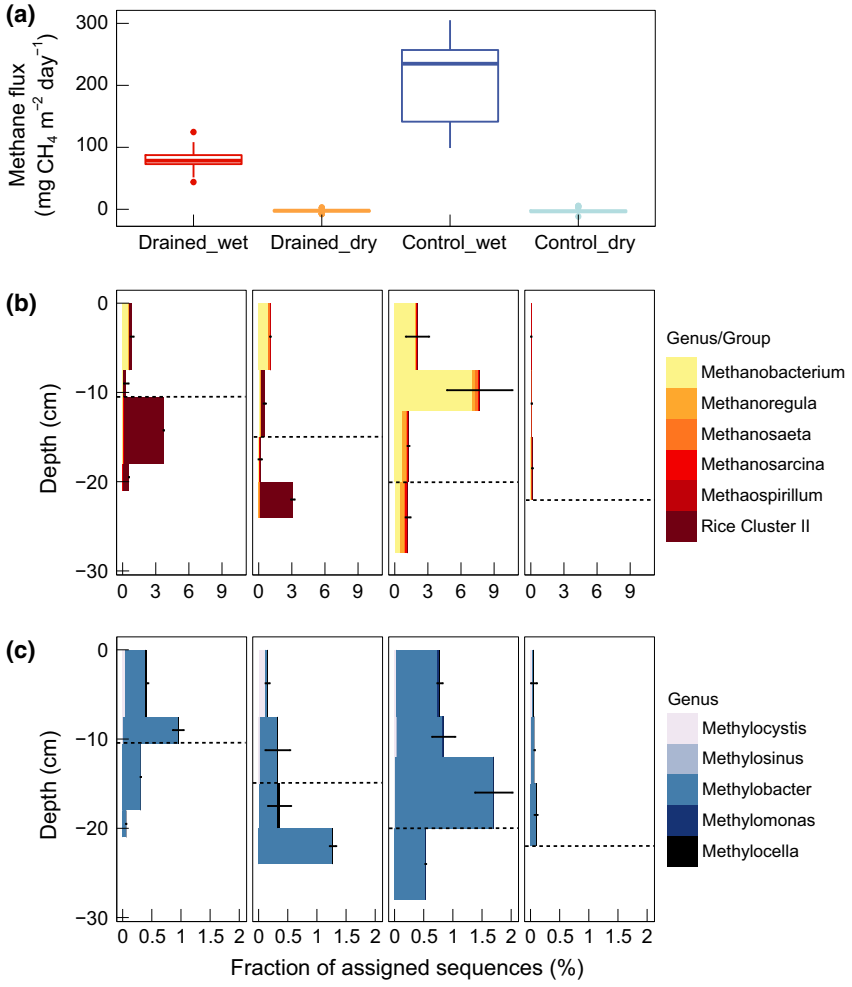

Fig. 4 CH_4 fluxes and the fractions of CH_4-related microorganisms. (a) CH_4 fluxes at four plots where microbial samples were taken. The fractions of (b) methanogenic and (c) methanotrophic groups by depth. Dashed lines indicate the borders between organic and mineral soil layers. [Colour figure can be viewed at wileyonlinelibrary.com].

Methanobacterium was prevalent in the control transect, while Rice Cluster II was dominant in the drained transect, especially in deeper soil layers (Table S2, Fig. 4b).

Methanotrophs were relatively most abundant in control_wet plots and relatively least abundant in control_dry plots (Fig. 4c). This difference by water table was substantial when the relative abundance of the two uppermost soil layers was compared (two-way ANOVA; drainage, $F = 0.09$, $P = 0.76$; water, $F = 44.34$, $P < 0.001$; drainage × water, $F = 4.22$, $P = 0.06$). Significant differences were also found in community composition between water table categories (two-way PERMANOVA; drainage, $F = 1.66$, $P = 0.19$; water, $F = 16.93$, $P < 0.001$; drainage × water, $F = 2.37$, $P = 0.10$). *Methylobacter* was the most common group at all depths of all plots, and *Methylocystis* was relatively most abundant at the surface layers (Table S3, Fig. 4c).

The quantities of bacteria were 85% and 75% higher under dry conditions than in wet conditions in the drained and the control transects, respectively (two-way ANOVA; drainage, $F = 26.75$, $P < 0.001$; water, $F = 23.81$, $P < 0.001$; drainage × water, $F = 2.76$, $P = 0.11$; Fig. S3), but the abundance of archaea did not

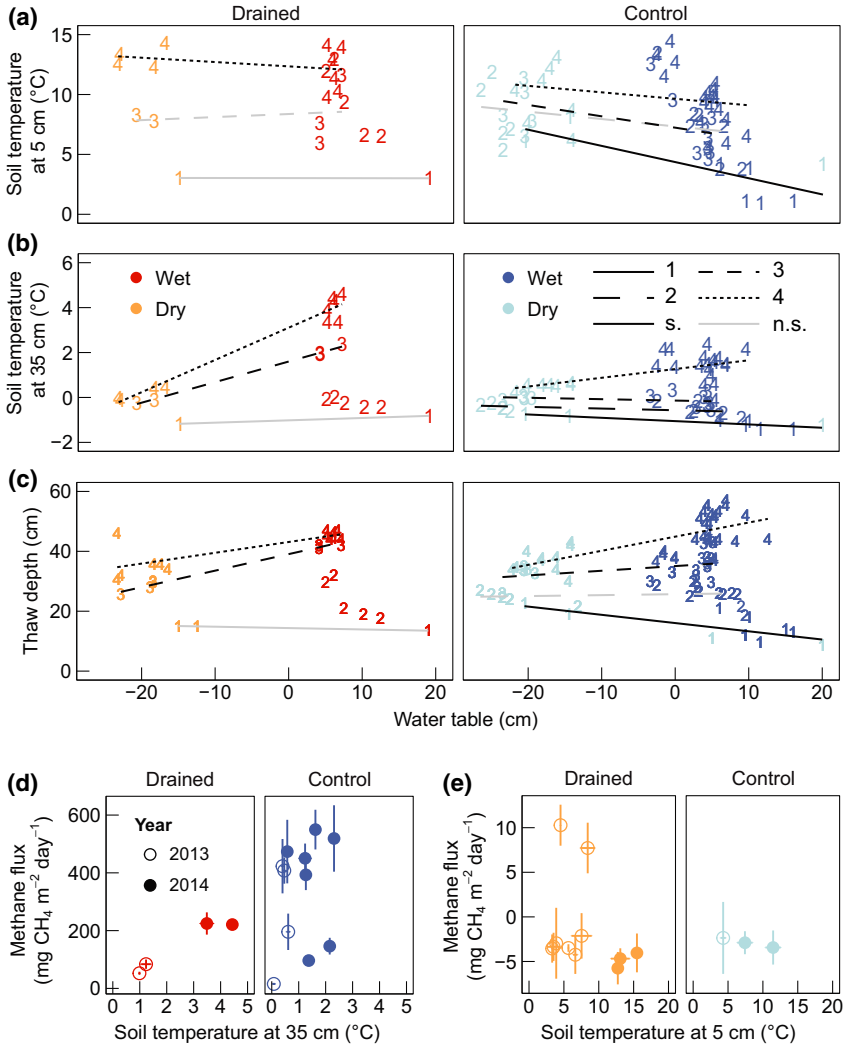

Fig. 5 T_{soil} at (a) 5 cm and (b) 35 cm, and (c) TD against water table, and their relations to growing-season CH_4 fluxes. Plots are based on the data from 2014 only, and those from dry plots that experienced rising water table following heavy precipitation events were excluded. Regression lines were drawn by subseason, and significance of regressions was indicated by color (black, $P < 0.05$; gray, not significant). Regression lines of Subseason 2 in the drained transect are missing due to limited information. Subseason 1 covers June 15 to 30, Subseason 2 July 1 to 15, Subseason 3 July 16 to 31, and Subseason 4 August 1 to 20. (d) Relationship between T_{soil} at 35 cm and CH_4 fluxes of the wet plots and (e) between T_{soil} at 5 cm and CH_4 fluxes of the dry plots. Data are from August to minimize seasonality and were grouped into temperature bins of 5 °C from 0 °C to 20 °C. Data from the dry plots with rising water table due to heavy precipitation were excluded. [Colour figure can be viewed at wileyonlinelibrary.com].

change between wet and dry areas (two-way ANOVA; drainage, $F = 2.11$, $P = 0.16$; water, $F = 0.50$, $P = 0.49$; drainage × water, $F = 9.33$, $P < 0.01$; Fig. S3).

The effects of T_{soil} and TD on growing-season CH_4 fluxes

The dry plots generally showed wider T_{soil} ranges vertically down to 35 cm compared to the wet plots: We found warmer T_{soil} in shallow soil layers during the daytime (linear regressions for Subseason 4; drained transect, $R^2 = 0.12$, $P < 0.01$; control transect, $R^2 = 0.06$, $P < 0.01$; Fig. 5a), but colder T_{soil} in deep soil layers (linear regressions for Subseason 4; drained transect, $R^2 = 0.97$, $P < 0.001$; control transect, $R^2 = 0.36$, $P < 0.001$; Fig. 5b). We also found there to be shallower TD in drier plots than in wet plots (linear regressions for the Subseason 4; drained transect, $R^2 = 0.61$, $P < 0.001$; control transect, $R^2 = 0.48$, $P < 0.001$; Fig. 5c). These trends became more distinct in the later subseasons (Fig. 5a–c).

T_{soil} at 35 cm in the wet plots positively related to growing-season CH_4 fluxes (linear regressions for August; drained transect, $R^2 = 0.93$, $P < 0.001$; control transect, $R^2 = 0.11$, $P < 0.001$; Fig. 5d). At the same time, T_{soil} in shallow layers of the dry plots negatively correlated with growing-season CH_4 fluxes (linear regressions for August; drained transect, $R^2 = 0.04$, $P < 0.05$; control transect, $R^2 = 0.00$, $P = 0.32$; Fig. 5e). It should be noted that CH_4 production and oxidation rates were not estimated in this study and that the interpretation of these correlations was based on the assumption that (1) CH_4 production occurs predominantly in deep soil layers with more anaerobic condition, while (2) CH_4 oxidation happens more in shallow layers with more aerobic condition. It is also assumed that (3) CH_4 fluxes of the wet plots are dominated by CH_4 production or are less affected by CH_4 oxidation and that CH_4 fluxes within the dry plots are largely influenced by CH_4 oxidation.

Plant community structure and its effects on growing-season CH_4 fluxes

In 2003 – before the drainage ditch was installed in 2004 – *E. angustifolium* was the most dominant species (Corradi *et al.*, 2005). Ten years after the drainage ditch was installed, the abundance of *E. angustifolium* in the drained transect was significantly lower than in the control transect (one-way ANOVA; $F = 3.97$, $P < 0.05$; Fig. 6a). Other aerenchymatous plants, *C. appendiculata* and *P. palustris,* showed no significant differences in abundance between the two transects (one-way ANOVA; *C. appendiculata*, $P = 0.32$; *P. palustris*, $P = 0.82$).

CH_4 fluxes and *E. angustifolium* cover were positively correlated, although each site category showed varying flux rates (linear regressions for August; drained transect, $R^2 = 0.78$, $P < 0.001$; control transect, $R^2 = 0.48$, $P < 0.001$; Fig. 6b). One plot that belonged to the drained_dry category and had abundant *E. angustifolium* showed relatively higher CH_4 fluxes compared to the rest of the same group despite low water table (Fig. 2b). Moreover, one plot in control_wet group covered only by *C. appendiculata* had significantly lower CH_4 fluxes compared to the plots covered by *E. angustifolium*, despite the presence of wet conditions in both plots (Fig. 2b). Contribution of the other aerenchymatous species present in the site – *P. palustris* – was approximately an order of magnitude lower than that of *E. angustifolium* (data not shown).

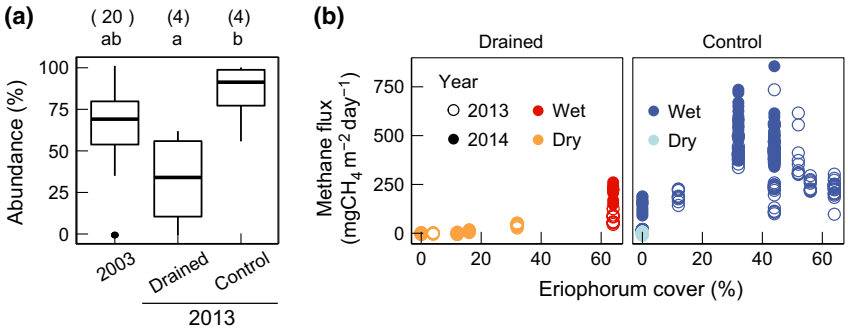

Fig. 6 Abundance of *Eriophorum angustifolium* and its effect on CH_4 fluxes. (a) Abundance of *E. angustifolium*, with 25% and 75% quartiles and ±1.5 interquartile ranges. Numbers in parentheses are the number of observations. Significance of differences between groups (determined by one-way ANOVA and Tukey's *post hoc* test) is indicated by the letters. Different letters denote significant differences among groups, while the same letters indicate a lack of significant difference. (b) Relation between *E. angustifolium* cover and CH_4 fluxes. Results are restricted to data from August to minimize temporal variability in fluxes. [Colour figure can be viewed at wileyonlinelibrary.com].

Discussion

Microbial effects

Larger fractions of CH_4-associated microorganisms coincided with greater CH_4 fluxes, indicating that CH_4 cycling was more pronounced under wetter conditions. High soil water contents favoring anoxic conditions led to larger populations of methanogens, and their continuous production of CH_4 maintained methanotrophic populations similar to other studies (Liebner & Wagner, 2007; Mayumi *et al*., 2010). In addition, as depth increased, larger fractions of CH_4-related microbial groups were found in the drained transect, mostly within or close to mineral soil layers, where carbon content was significantly lower than in organic layers. Thus, although the sum of the fractions of both microbial groups in the drained transect was similar to control_wet, the smaller amount of carbon in deeper layers can potentially result in reduced CH_4 cycling due to the dependence of methanogenic activity on abundant labile carbon substrates (Deppe *et al*., 2010; Klapstein *et al*., 2014). Furthermore, with hot spots of CH_4 cycling existing in deeper layers in drained soils, a higher proportion of CH_4 can be oxidized at shallower, more aerated soil depths (Frenzel *et al*., 1992; Sass *et al*., 1992), which may have larger abundance of CH_4-oxidizers. This larger abundance can be inferred from the increased quantity of bacteria. Although, due to our limited number of samples, we did not attempt to quantitatively relate microbial communities to CH_4 fluxes, abundant fractions of CH_4-associated microorganisms in deeper soil layers may explain the reduced CH_4 fluxes in the drained transect, especially in drained_wet, despite having a similar water table to that of control_wet.

Not only the relative abundance, but also the microbial composition differed between the four soil groups. Although remains challenging to assess structure and function relationships in CH_4 cycling microbial groups, due to the lack of information on the physiology of known microorganisms in soils and their ability to acclimate to changing environments (Tveit *et al*., 2015), the processes and genetic markers infer linkage between microbial community structure and CH_4 cycling (Høj *et al*., 2006; McCalley *et al*., 2014; Christiansen *et al*., 2015; Hultman *et al*., 2015). For instance, an increased relative abundance of the known methanotroph *Methylocystis* (which can oxidize CH_4 at both high and low concentrations; Baani & Liesack, 2008) in shallow layers of the dry plots (Table S3) suggests that its spatial niche has expanded in the soil following drainage: Within these layers, methanotrophs can then oxidize atmospheric CH_4, thereby potentially strengthening the CH_4 sink capacity of this ecosystem. Although quantitative relations between microbial communities and CH_4 fluxes could not be found, significantly changed abundances and compositions of CH_4-related microorganisms following long-term drainage (Fig. 4b and c) may have dramatic effects on CH_4 cycling in this ecosystem.

T_{soil} effects

Another factor that influences CH_4 production and oxidation rates is T_{soil}, because both processes are thermodynamically influenced, with their rates increasing with temperature up to their optimal temperatures (Dunfield *et al*., 1993; Westermann, 1993; Whalen & Reeburgh, 1996; Yvon-Durocher *et al*., 2014). Dry organic soils can be easily heated and cooled due to their lower heat capacity (Idso *et al*., 1975; Reginato *et al*., 1976; Abu-Hamdeh, 2003; Lakshmi *et al*., 2003). Dry soils also poorly transfer heat to the surrounding areas due to their low thermal conductivity (Abu-Hamdeh, 2003). Thus, T_{soil} in shallow layers in the dry plots fluctuated across a wide temperature range (Fig. 5a), and T_{soil} in deep layers was colder (Fig. 5b), with shallower TDs (Fig. 5c) compared to the wet plots. This divergence of T_{soil} was linked to CH_4 production and oxidation rates in deep and shallow layers, respectively: Warmer T_{soil} in shallow layers and colder T_{soil} in deep layers in the drained areas both contributed to a decrease in net CH_4 fluxes (Fig. 5d and e) due to potentially reduced rates of methanogenesis and increased rates of CH_4 oxidation. Unlike microbial community structures, which require time to acclimate to changed conditions, T_{soil} can be immediately affected by soil moisture, and changes in it due to climate (e.g., precipitation) can instantly intensify or dampen T_{soil} effects on rates of CH_4 processes.

Plant effects

Aside from the microbially mediate production and consumption of CH_4, gas transport pathways have the potential to impact CH_4 flux rates (Kutzbach *et al*., 2004; von Fischer *et al*., 2010; Knoblauch *et al*., 2015; Andresen *et al*., 2016). Three aerenchymatous plant species exist in this study site: *C. appendiculata*, *P. palustris*, and *E. angustifolium*. Similar CH_4 flux rates were found in *Carex*-dominated and in *Eriophorum*- and *Potentilla*-dominated areas under saturated conditions in a previous study (Corradi *et al*., 2005), implying that three species transport CH_4 through aerenchyma. However, in this study, *E. angustifolium* appeared to facilitate more CH_4 transport in

comparison with *C. appendiculata* and *P. palustris* (Figs 2b and 6b, Eqn 4). A negative influence of *C. appendiculata* cover on growing-season CH_4 fluxes observed in the drained transect (Eqn 3) can be attributed to its dominance in drained plots, where CH_4 production rate is low, and partly due to its tussock structure (dense rhizomes), where a large fraction of CH_4 can be potentially oxidized (Nishikawa, 1990; Bosse & Frenzel, 1997; Le Mer & Roger, 2001). Even though the contribution of aerenchyma to CH_4 fluxes on this Arctic floodplain was lower than in other studies of Arctic tundra (Kutzbach *et al.*, 2004; Knoblauch *et al.*, 2015), *E. angustifolium* transported a significant amount of CH_4 from deep soils to the atmosphere under naturally wet conditions, in strong agreement with previous knowledge (Fig. 6b; Chanton & Dacey, 1991; Kutzbach *et al.*, 2004; von Fischer *et al.*, 2010; Knoblauch *et al.*, 2015). However, persistently low water table (due to drainage) for 10 years decreased the abundance of *E. angustifolium* and thus the possibility of directly transporting CH_4 to the atmosphere (Fig. 6). A large amount of CH_4 that would otherwise reach the atmosphere through aerenchyma prior to drainage was shunted through aerobic soil layers, where it had an increased probability of undergoing oxidation.

The observed plant community structures in the control transect show that the relative abundance of plant species in the study area depends on the adaptation of each species to long-term conditions, such as soil moisture (Luo *et al.*, 2008): *E. angustifolium* dominated in the wet plots, while no *E. angustifolium* was found in the dry plots. After decade-long drainage, several drained_dry plots displayed a transition in the plant community, resulting in limited *E. angustifolium* cover and young *C. appendiculata*. Both *E. angustifolium* and *C. appendiculata* are abundant in wetlands due to aerenchyma structures that enable adaptation to water-saturated conditions (Jackson & Armstrong, 1999; Crawford, 2013), but the presence of this transitional community implies that drainage lowered the productivity of *E. angustifolium* – which are less adaptive to dry conditions, but not *C. appendiculata* – which are more tolerant to fluctuating water table of drained floodplain due to tussock structure (Crawford, 2013). Despite the decreased abundance of *E. angustifolium*, a small amount of CH_4 was transported through the remaining *E. angustifolium* in drained_dry plots, with a further decrease in the abundance of *E. angustifolium* expected in these plots with continued drainage. As this change takes place, the amount of CH_4 transported through aerenchyma will be further reduced and net CH_4 fluxes may become similar to those in control_dry plots.

Growing-season CH_4 fluxes

The average daily CH_4 fluxes were 10–11 mg CH_4 m^{-2} day^{-1} in the drained and 213–265 mg CH_4 m^{-2} day^{-1} in the control transects after 10 years of drainage. This range was comparable to that observed in a previous study conducted at the same site in 2002–2005: 247–296 and 7 mg CH_4 m^{-2} day^{-1} before and after the drainage ditch was installed, respectively (Corradi *et al.*, 2005; Merbold *et al.*, 2009). Differences in the flux rates between the studies may be due in part to the different observation periods chosen: The 2002–2005 field campaigns ran 16 July to 31 October, while the 2013–2014 field campaigns covered from mid-June or mid-July up to 20 August. The significant reduction in CH_4 fluxes 1 year after the installation of the drainage ditch implies that a decrease in water table – which caused more aerobic conditions – considerably affected growing-season CH_4 fluxes (Merbold *et al.*, 2009). However, without changes in ecosystem properties, the growing-season CH_4 fluxes would have been expected to be restored a few days to a month after water table was raised, such as following heavy precipitation events (Yagi *et al.*, 1996; Boon *et al.*, 1997; Ratering & Conrad, 1998; Deppe *et al.*, 2010). Ten years after the drainage installation, the decreased growing-season CH_4 flux rates remained at similar levels. This reduction was likely triggered by changes to ecosystem properties that impacted CH_4 flux rates including the following: the fractions of CH_4-associated microorganisms, T_{soil}, and abundances of *E. angustifolium*. Given these modified ecosystem properties, an instant rise in water table would be unlikely to restore CH_4 flux rates to the original high rates (Komulainen *et al.*, 1998; Waddington & Day, 2007). Besides these three factors, P_a negatively influenced growing-season CH_4 fluxes (Eqns 3 and 4) with low or descending P_a triggering CH_4 emissions due to the diminished pressure on soils (Mattson & Likens, 1990; Tokida *et al.*, 2007; Sachs *et al.*, 2010). Our results indicate that biotic and abiotic parameters besides water table (Eqns 3 and 4) are critical in controlling growing-season CH_4 fluxes. Moreover, due to altered CH_4 transport pathways following drainage – a larger proportion of CH_4 was likely transported through diffusion to aerobic soils (Table 2) – resulting in an increased probability of oxidation. The results of this study highlight the role of microorganisms, T_{soil}, and plants in regulating CH_4 fluxes – along with water table – and stress the importance of long-term studies that can observe shifts in these ecosystem properties.

Nongrowing season CH_4 fluxes

Low or decreasing P_a may have affected high CH_4 fluxes, while *E. angustifolium* acted as a pathway for CH_4 transport in the nongrowing seasons. These controlling factors (Eqns 5 and 6) were similar to those in the growing season (Eqns 3 and 4), but variability in fluxes during the nongrowing season was considerably higher compared to those in the growing season. In addition, higher CH_4 fluxes at each site in the growing season did not translate to higher CH_4 fluxes in the nongrowing season. This may be partly attributed to the limited availability of liquid water and the physical barrier of the frozen soil matrix that constrained CH_4 production, oxidation, and transport processes during the nongrowing season. In addition, gradual freezing soil can push stored CH_4 gas from soils to the atmosphere (Mastepanov *et al.*, 2008, 2013), and this effect may have been stronger in compacted dry soils following drainage. Thus, nongrowing-season CH_4 fluxes were more influenced by physical than biological factors, showing similar sporadic fluxes as reported in previous studies (Whalen & Reeburgh, 1992; Mastepanov *et al.*, 2008, 2013; Wille *et al.*, 2008; Zona *et al.*, 2015). Despite significant physical effects on CH_4 fluxes in the nongrowing season, mild T_{soil} compared to T_a should not be overlooked, which could well support CH_4 production. Mean T_{soil} at 35 cm during this observation period was −5 °C and −6 °C for wet and dry plots, respectively; these temperatures were approximately 17 °C warmer than the mean T_a of −22 °C. The amount of CH_4 that can be produced under these temperatures (−5 °C and −6 °C) is not negligible (Rivkina *et al.*, 2004, 2007), especially considering the fact that the nongrowing season is approximately three times longer compared to the growing season in the Arctic.

During the growing season, CH_4 fluxes were 19–28 times lower following drainage. This difference was slightly offset by 10% higher CH_4 emissions in early winter, although higher CH_4 emission rates in the drained transect were largely driven by the drained_wet plot, which was marginally drained and dominated by *E. angustifolium*. This indicates that, in the future, CH_4 emissions in the drained transect may continue to fall with continuing drainage and a decreasing abundance of *E. angustifolium*. As irregular fluxes are frequently observed (Mastepanov *et al.*, 2008, 2013; Wille *et al.*, 2008; Zona *et al.*, 2015), and the nongrowing season in the Arctic is roughly three times longer than the growing season, continuous monitoring of CH_4 fluxes in the nongrowing season is necessary to completely elucidate the net effects of drainage on the CH_4 fluxes in this ecosystem. Nevertheless, given the variable but significant CH_4 fluxes observed, our study highlights the potential importance of the nongrowing season's contributions to annual CH_4 fluxes.

To summarize, our drying manipulation experiment, whereby we mimicked the drainage that would accompany ice-rich permafrost thaw and ground subsidence in the Arctic, showed that 10 years of dry conditions in Arctic wetlands altered CH_4-related microbial community structure, soil thermal regimes, and plant community structure and that these modifications contributed to a considerable decrease in CH_4 fluxes by altering CH_4 production, oxidation, and transport processes. Given these ecosystem changes, momentary water table rise due to heavy precipitation would not restore CH_4 fluxes to the original level. Continuing dry conditions may further reduce CH_4 fluxes by causing ongoing changes in the vegetation community. While CH_4 fluxes are expected to rise along with degraded permafrost, due to warmer and wetter conditions in the Arctic (Christensen & Cox, 1995; Oberbauer *et al.*, 1998; Walter *et al.*, 2006), implementing drainage in the event of thawing permafrost can counterbalance this effect.

Acknowledgements

This work has been supported by the European Commission (PAGE21 project, FP7-ENV-2011, grant agreement no. 282700; PerCCOM project, FP7-PEOPLE-2012-CIG, grant agreement no. PCIG12-GA-2012-333796), the German Ministry of Education and Research (CarboPerm-Project, BMBF grant no. 03G0836G), the International Max Planck Research School for Global Biogeochemical Cycles (IMPRS-gBGC), and the AXA Research Fund (PDOC_2012_W2 campaign, ARF fellowship M. Göckede). The contributions of J. E. Kostka were supported by the Terrestrial Ecosystem Science (TES) Program, under U. S. Department of Energy contracts DE-SC0007144 and DE-SC0012088. The authors appreciate NESS staff members, especially Galina Zimova, Nastya Zimova, and Vladimir Tatayev for organizing and assisting with field work; Chiara Corradi for providing us a historic dataset and valuable advice; Martin Hertel, Frank Voigt, Waldemar Ziegler, and Freiland group members for technical support; Ina Burjack for providing an aerial map (Fig. 1) and for assisting with field and laboratory work; Mirco Migliavacca for advice on data analysis; Cassandre Sara Lazar for methanogen identification; Patricia Lange for quantifying bacteria and archaea; and Julia L. McMillan for the language editing. We ordered our authors according to both the first–last author emphasis and sequence–determined–credit methods (Tscharntke *et al.*, 2007).

Data accessibility

DNA sequences are available from European Nucleotide Archive (ENA; Study accession number: PRJEB14835).

References

Abu-Hamdeh NH (2003) Thermal properties of soils as affected by density and water content. *Biosystems Engineering*, **86**, 97–102.

Andresen CG, Lara MJ, Tweedie CE, Lougheed VL (2016) Rising plant-mediated methane emissions from Arctic wetlands. *Global Change Biology*. doi: 10.1111/gcb.13469.

Aselmann I, Crutzen PJ (1989) Global distribution of natural freshwater wetlands and rice paddies, their net primary productivity, seasonality and possible methane emissions. *Journal of Atmospheric Chemistry*, **8**, 307–358.

Baani M, Liesack W (2008) Two isozymes of particulate methane monooxygenase with different methane oxidation kinetics are found in Methylocystis sp. strain SC2. *Proceedings of the National Academy of Sciences of the United States of America*, **105**, 10203–10208.

Batjes NH (1996) Total carbon and nitrogen in the soils of the world. *European Journal of Soil Science*, **47**, 151–163.

Bintanja R, Selten FM (2014) Future increases in Arctic precipitation linked to local evaporation and sea-ice retreat. *Nature*, **509**, 479–482.

Bonin AS, Boone DR (2006) The order methanobacteriales. In: *The Prokaryotes* (eds. Dworkin M, Falkow S, Rosenberg E, Schleifer K-H, Stackebrandt E), pp. 231–243. Springer, New York, NY.

Boon PI, Mitchell A, Lee K (1997) Effects of wetting and drying on methane emissions from ephemeral floodplain wetlands in south-eastern Australia. *Hydrobiologia*, **357**, 73–87.

Bosse U, Frenzel P (1997) Activity and distribution of methane-oxidizing bacteria in flooded rice soil microcosms and in rice plants (Oryza sativa). *Applied and Environmental Microbiology*, **63**, 1199–1207.

Bowman J (2006) The methanotrophs – the families methylococcaceae and methylocystaceae. In: *The Prokaryotes* (eds. Dworkin M, Falkow S, Rosenberg E, Schleifer K-H, Stackebrandt E), pp. 266–289. Springer, New York, NY.

Bräuer SL, Cadillo-Quiroz H, Yashiro E, Yavitt JB, Zinder SH (2006) Isolation of a novel acidiphilic methanogen from an acidic peat bog. *Nature*, **442**, 192–194.

Caporaso JG, Lauber CL, Walters WA *et al*. (2011) Global patterns of 16S rRNA diversity at a depth of millions of sequences per sample. *Proceedings of the National Academy of Sciences of the United States of America*, **108**, 4516–4522.

Caporaso JG, Lauber CL, Walters WA *et al*. (2012) Ultra-high-throughput microbial community analysis on the Illumina HiSeq and MiSeq platforms. *ISME Journal*, **6**, 1621–1624.

Chanton JP, Dacey JWH (1991) Effects of vegetation on methane flux, reservoirs, and carbon isotopic composition. In: *Trace gas Emissions by Plants* (eds Sharkey TD, Holland EA, Mooney HA), pp. 65–92. Academic Press Inc, San Diego, CA.

Christensen TR, Cox P (1995) Response of methane emission from Arctic tundra to climate change: results from a model simulation. *Tellus*, **47B**, 301–309.

Christiansen JR, Romero AJB, Jørgensen NOG, Glaring MA, Jørgensen CJ, Berg LK, Elberling B (2015) Methane fluxes and the functional groups of methanotrophs and methanogens in a young Arctic landscape on Disko Island, West Greenland. *Biogeochemistry*, **122**, 15–33.

Ciais P, Sabine C, Bala G *et al*. (2013) Carbon and other biogeochemical cycles. In: *Climate Change 2013: The Physical Science Basis. Contribution of Working Group I to the Fifth Assessment Report of the Intergovernmental Panel on Climate Change* (eds. Stocker TF, Qin D, Plattner G-K, Tignor MMB, Allen SK, Boschung J, Nauels A, Xia Y, Bex V, Midgley PM), pp. 465–570. Cambridge University Press, Cambridge, UK and New York, NY.

Coello CA, Montes EM (2002) Constraint-handling in genetic algorithms through the use of dominance-based tournament selection. *Advanced Engineering Informatics*, **16**, 193–203.

Collins M, Knutti R, Arblaster J *et al*. (2013) Long-term climate change: projections, commitments and irreversibility. In: *Climate Change 2013: The Physical Science Basis. Contribution of Working Group I to the Fifth Assessment Report of the Intergovernmental Panel on Climate Change* (eds. Stocker TF, Qin D, Plattner G-K, Tignor MMB, Allen SK, Boschung J, Nauels A, Xia Y, Bex V, Midgley PM), pp. 1029–1136. Cambridge University Press, Cambridge and New York, NY.

Corradi C, Kolle O, Walter K, Zimov SA, Schulze ED (2005) Carbon dioxide and methane exchange of a north-east Siberian tussock tundra. *Global Change Biology*, **11**, 1910–1925.

Crawford RMM (2013) Tundra diversity. In: *Tundra-Taiga Biology* pp. 70–92. Oxford University Press, Oxford.

Curtis J, Wendler G, Stone R, Dutton E (1998) Precipitation decrease in the western Arctic, with special emphasis on Barrow and Barter Island, Alaska. *International Journal of Climatology*, **18**, 1687–1707.

Daims H, Brühl A, Amann R, Schleifer K-H, Wagner M (1999) The domain-specific probe EUB338 is insufficient for the detection of all bacteria: development and evaluation of a more comprehensive probe set. *Systematic and Applied Microbiology*, **22**, 434–444.

Danilova OV, Kulichevskaya IS, Rozova ON, Detkova EN, Bodelier PLE, Trotsenko YA, Dedysh SN (2013) Methylomonas paludis sp. nov., the first acid-tolerant member of the genus Methylomonas, from an acidic wetland. *International Journal of Systematic and Evolutionary Microbiology*, **63**, 2282–2289.

Dedysh SN, Liesack W, Khmelenina VN *et al*. (2000) Methylocella palustris gen. nov., sp. nov., a new methane-oxidizing acidophilic bacterium from peat bogs, representing a novel subtype of serine-pathway methanotrophs. *International Journal of Systematic and Evolutionary Microbiology*, **50**, 955–969.

Dedysh SN, Berestovskaya YY, Vasylieva LV *et al*. (2004) Methylocella tundrae sp. nov., a novel methanotrophic bacterium from acidic tundra peatlands. *International Journal of Systematic and Evolutionary Microbiology*, **54**, 151–156.

DeLong EF (1992) Archaea in coastal marine environments. *Proceedings of the National Academy of Sciences of the United States of America*, **89**, 5685–5689.

Deppe M, Knorr K-H, McKnight DM, Blodau C (2010) Effects of short-term drying and irrigation on CO_2 and CH_4 production and emission from mesocosms of a northern bog and an alpine fen. *Biogeochemistry*, **100**, 89–103.

Dunfield P, Knowles R, Dumont R, Moore T (1993) Methane production and consumption in temperate and subarctic peat soils: response to temperature and pH. *Soil Biology and Biochemistry*, **25**, 321–326.

Dunfield PF, Yimga MT, Dedysh SN, Berger U, Liesack W, Heyer J (2002) Isolation of a Methylocystis strain containing a novel pmoA-like gene. *FEMS Microbiology Ecology*, **41**, 17–26.

Dunfield PF, Khmelenina VN, Suzina NE, Trotsenko YA, Dedysh SN (2003) *Methylocella silvestris* sp. nov., a novel methanotroph isolated from an acidic forest cambisol. *International Journal of Systematic and Evolutionary Microbiology*, **53**, 1231–1239.

Edgar RC, Haas BJ, Clemente JC, Quince C, Knight R (2011) UCHIME improves sensitivity and speed of chimera detection. *Bioinformatics (Oxford, England)*, **27**, 2194–2200.

Ferreira C (2001) Gene expression programming: a new adaptive algorithm. In: *The 6th Online World Conference on Soft Computing in Industrial Applications*.

von Fischer JC, Rhew RC, Ames GM, Fosdick BK, von Fischer PE (2010) Vegetation height and other controls of spatial variability in methane emissions from the Arctic coastal tundra at Barrow, Alaska. *Journal of Geophysical Research: Biogeosciences*, **115**, G00I03.

Frenzel P, Rothfuss F, Conrad R (1992) Oxygen profiles and methane turnover in a flooded rice microcosm. *Biology and Fertility of Soils*, **14**, 84–89.

Garcia J-L, Ollivier B, Whitman WB (2006) The order methanomicrobiales. In: *The Prokaryotes* (eds. Dworkin M, Falkow S, Rosenberg E, Schleifer K-H, Stackebrandt E), pp. 208–230. Springer, New York, NY.

Gilbert JA, Jansson JK, Knight R *et al*. (2014) The Earth Microbiome Project: successes and aspirations. *BMC Biology*, **12**, 69.

Großkopf R, Stubner S, Liesack W (1998) Novel euryarchaeotal lineages detected on rice roots and in the anoxic bulk soil of flooded rice cicrocosms. *Applied and Environmental Microbiology*, **64**, 4983–4989.

Hansen N, Müller SD, Koumoutsakos P (2003) Reducing the time complexity of the derandomized evolution strategy with covariance matrix adaptation (CMA-ES). *Evolutionary Computation*, **11**, 1–18.

Hanson RS, Hanson TE (1996) Methanotrophic bacteria. *Microbiological Reviews*, **60**, 439–471.

Hedderich R, Whitman WB (2013) Physiology and biochemistry of the methane-producing archaea. In: *The Prokaryotes* (eds. Rosenberg E, DeLong EF, Lory S, Stackebrandt E, Thompson F), pp. 635–662. Springer, Berlin Heidelberg.

Herrmann M, Hädrich A, Küsel K (2012) Predominance of thaumarchaeal ammonia oxidizer abundance and transcriptional activity in an acidic fen. *Environmental Microbiology*, **14**, 3013–3025.

Høj L, Rusten M, Haugen LE, Olsen RA, Torsvik VL (2006) Effects of water regime on archaeal community composition in Arctic soils. *Environmental Microbiology*, **8**, 984–996.

Hugelius G, Strauss J, Zubrzycki S *et al*. (2014) Estimated stocks of circumpolar permafrost carbon with quantified uncertainty ranges and identified data gaps. *Biogeosciences*, **11**, 6573–6593.

Hultman J, Waldrop MP, Mackelprang R *et al*. (2015) Multi-omics of permafrost, active layer and thermokarst bog soil microbiomes. *Nature*, **521**, 208–212.

Huntington TG (2006) Evidence for intensification of the global water cycle: review and synthesis. *Journal of Hydrology*, **319**, 83–95.

Idso SB, Schmugge TJ, Jackson RD, Reginato RJ (1975) The utility of surface temperature measurements for the remote sensing of surface soil water status. *Journal of Geophysical Research*, **80**, 3044–3049.

Jackson MB, Armstrong W (1999) Formation of aerenchyma and the processes of plant ventilation in relation to soil flooding and submergence. *Plant Biology*, **1**, 274–287.

Jobbágy EG, Jackson RB (2000) The vertical distribution of soil organic carbon and its relation to climate and vegetation. *Ecological Applications*, **10**, 423–436.

Jorgenson MT, Shur YL, Pullman ER (2006) Abrupt increase in permafrost degradation in Arctic Alaska. *Geophysical Research Letters*, **33**, L02503.

Kattsov VM, Walsh JE (2000) Twentieth-century trends of Arctic precipitation from observational data and a climate model simulation. *Journal of Climate*, **13**, 1362–1370.

Kendall MM, Boone DR (2006) The order methanosarcinales. In: *The Prokaryotes* (eds. Dworkin M, Falkow S, Rosenberg E, Schleifer K-H, Stackebrandt E), pp. 244–256. Springer, New York, NY.

Kim Y (2015) Effect of thaw depth on fluxes of CO_2 and CH_4 in manipulated Arctic coastal tundra of Barrow, Alaska. *The Science of the Total Environment*, **505**, 385–389.

King JY, Reeburgh WS, Regli SK (1998) Methane emission and transport by arctic sedges in Alaska: results of a vegetation removal experiment. *Journal of Geophysical Research*, **103**, 29083–29092.

Kirschke S, Bousquet P, Ciais P *et al.* (2013) Three decades of global methane sources and sinks. *Nature Geoscience*, **6**, 813–823.

Kirtman B, Power SB, Adedoyin JA *et al.* (2013) Near-term climate change: projections and predictability. In: *Climate Change 2013: The Physical Science Basis. Contribution of Working Group I to the Fifth Assessment Report of the Intergovernmental Panel on Climate Change* (eds. Stocker TF, Qin D, Plattner G-K, Tignor MMB, Allen SK, Boschung J, Nauels A, Xia Y, Bex V, Midgley PM), pp. 953–1028. Cambridge University Press, Cambridge and New York, NY.

Kittler F, Burjack I, Corradi CAR *et al.* (2016) Impacts of a decadal drainage disturbance on surface–atmosphere fluxes of carbon dioxide in a permafrost ecosystem. *Biogeosciences*, **13**, 5315–5332.

Klapstein SJ, Turetsky MR, McGuire AD *et al.* (2014) Controls on methane released through ebullition in peatlands affected by permafrost degradation. *Journal of Geophysical Research: Biogeosciences*, **119**, 418–431.

Knoblauch C, Spott O, Evgrafova S, Kutzbach L, Pfeiffer E-M (2015) Regulation of methane production, oxidation and emission by vascular plants and bryophytes in ponds of the northeast Siberian polygonal tundra. *Journal of Geophysical Research: Biogeosciences*, **120**, 2525–2541.

Komulainen V-M, Nykänen H, Martikainen PJ, Laine J (1998) Short-term effect of restoration on vegetation change and methane emissions from peatlands drained for forestry in southern Finland. *Canadian Journal of Forest Research*, **28**, 402–411.

Kutzbach L, Wagner D, Pfeiffer E-M (2004) Effect of microrelief and vegetation on methane emission from wet polygonal tundra, Lena Delta, Northern Siberia. *Biogeochemistry*, **69**, 341–362.

Lakshmi V, Jackson TJ, Zehrfuhs D (2003) Soil moisture-temperature relationships: results from two field experiments. *Hydrological Processes*, **17**, 3041–3057.

Le Mer J, Roger P (2001) Production, oxidation, emission and consumption of methane by soils: a review. *European Journal of Soil Biology*, **37**, 25–50.

Liebner S, Wagner D (2007) Abundance, distribution and potential activity of methane oxidizing bacteria in permafrost soils from the Lena Delta, Siberia. *Environmental Microbiology*, **9**, 107–117.

Loy A, Lehner A, Lee N *et al.* (2002) Oligonucleotide microarray for 16S rRNA gene-based detection of all recognized lineages of sulfate-reducing prokaryotes in the environment. *Applied and Environmental Microbiology*, **68**, 5064–5081.

Luo W, Song F, Xie Y (2008) Trade-off between tolerance to drought and tolerance to flooding in three wetland plants. *Wetlands*, **28**, 866–873.

Mastepanov M, Sigsgaard C, Dlugokencky EJ, Houweling S, Ström L, Tamstorf MP, Christensen TR (2008) Large tundra methane burst during onset of freezing. *Nature*, **456**, 628–630.

Mastepanov M, Sigsgaard C, Tagesson T, Ström L, Tamstorf MP, Lund M, Christensen TR (2013) Revisiting factors controlling methane emissions from high-Arctic tundra. *Biogeosciences*, **10**, 5139–5158.

Matthews E, Fung I (1987) Methane emission from natural wetlands: global distribution, area, and environmental characteristics of sources. *Global Biogeochemical Cycles*, **1**, 61–86.

Mattson MD, Likens GE (1990) Air pressure and methane fluxes. *Nature*, **347**, 718–719.

Mayumi D, Yoshimoto T, Uchiyama H, Nomura N, Nakajima-Kambe T (2010) Seasonal change in methanotrophic diversity and populations in a rice field soil assessed by DNA-stable isotope probing and quantitative real-time PCR. *Microbes and Environments*, **25**, 156–163.

McCalley CK, Woodcroft BJ, Hodgkins SB *et al.* (2014) Methane dynamics regulated by microbial community response to permafrost thaw. *Nature*, **514**, 478–481.

McEwing KR, Fisher JP, Zona D (2015) Environmental and vegetation controls on the spatial variability of CH_4 emission from wet-sedge and tussock tundra ecosystems in the Arctic. *Plant and Soil*, **388**, 37–52.

McGuire AD, Christensen TR, Hayes D *et al.* (2012) An assessment of the carbon balance of Arctic tundra: comparisons among observations, process models, and atmospheric inversions. *Biogeosciences*, **9**, 3185–3204.

Merbold L, Kutsch WL, Corradi C *et al.* (2009) Artificial drainage and associated carbon fluxes (CO_2/CH_4) in a tundra ecosystem. *Global Change Biology*, **15**, 2599–2614.

van der Molen MK, van Huissteden J, Parmentier FJW *et al.* (2007) The growing season greenhouse gas balance of a continental tundra site in the Indigirka lowlands, NE Siberia. *Biogeosciences*, **4**, 985–1003.

Mondav R, Woodcroft BJ, Kim E-H *et al.* (2014) Discovery of a novel methanogen prevalent in thawing permafrost. *Nature Communications*, **5**, 3212.

Morgenstern A, Ulrich M, Günther F *et al.* (2013) Evolution of thermokarst in East Siberian ice-rich permafrost: a case study. *Geomorphology*, **201**, 363–379.

Morrissey LA, Livingston GP (1992) Methane emissions from Alaska arctic tundra - an assessment of local spatial variability. *Journal of Geophysical Research-Atmospheres*, **97**, 16661–16670.

Nakano T, Kuniyoshi S, Fukuda M (2000) Temporal variation in methane emission from tundra wetlands in a permafrost area, northeastern Siberia. *Atmospheric Environment*, **34**, 1205–1213.

Nishikawa Y (1990) Role of rhizomes in tussock formation by Carex thunbergii var. Appendiculata. *Ecological Research*, **5**, 261–269.

Oberbauer SF, Starr G, Pop EW (1998) Effects of extended growing season and soil warming on carbon dioxide and methane exchange of tussock tundra in Alaska. *Journal of Geophysical Research*, **103**, 29075–29082.

O'Donnell JA, Jorgenson MT, Harden JW, McGuire AD, Kanevskiy MZ, Wickland KP (2011) The effects of permafrost thaw on soil hydrologic, thermal, and carbon dynamics in an Alaskan peatland. *Ecosystems*, **15**, 213–229.

Overland JE, Wang M, Walsh JE, Stroeve JC (2014) Future Arctic climate changes: adaptation and mitigation time scales. *Earth's Future*, **2**, 68–74.

R Development Core Team (2013) *R: A Language and Environment for Statistical Computing*. R Foundation for Statistical Computing, Vienna, Austria.

Ratering S, Conrad R (1998) Effects of short-term drainage and aeration on the production of methane in submerged rice soil. *Global Change Biology*, **4**, 397–407.

Reginato RJ, Idso SB, Vedder JF, Jackson RD, Blanchard MB, Goettelman R (1976) Soil water content and evaporation determined by thermal parameters obtained from ground-based and remote measurements. *Journal of Geophysical Research*, **81**, 1617–1620.

Rhew RC, Teh YA, Abel T (2007) Methyl halide and methane fluxes in the northern Alaskan coastal tundra. *Journal of Geophysical Research: Biogeosciences*, **112**, G02009.

Rivkina E, Laurinavichius K, McGrath J, Tiedje J, Shcherbakova V, Gilichinsky D (2004) Microbial life in permafrost. *Advances in Space Research: The Official Journal of the Committee on Space Research (COSPAR)*, **33**, 1215–1221.

Rivkina E, Shcherbakova V, Laurinavichius K *et al.* (2007) Biogeochemistry of methane and methanogenic archaea in permafrost. *FEMS Microbiology Ecology*, **61**, 1–15.

Rochette P, Hutchinson GL (2005) Measurement of soil respiration in situ: chamber techniques. *Micrometeorology in Agricultural Systems*, pp. 247–286. American Society of Agronomy, Madison, WI.

Sachs T, Giebels M, Boike J, Kutzbach L (2010) Environmental controls on CH_4 emission from polygonal tundra on the microsite scale in the Lena river delta, Siberia. *Global Change Biology*, **16**, 3096–3110.

Sass RL, Fisher FM, Wang YB, Turner FT, Jund MF (1992) Methane emission from rice fields: the effect of floodwater management. *Global Biogeochemical Cycles*, **6**, 249–262.

Schloss PDP, Westcott SSL, Ryabin T *et al.* (2009) Introducing mothur: open-source, platform-independent, community-supported software for describing and comparing microbial communities. *Applied and Environmental Microbiology*, **75**, 7537–7541.

Schuur EAG, McGuire AD, Schädel C *et al.* (2015) Climate change and the permafrost carbon feedback. *Nature*, **520**, 171–179.

Serreze MC, Barry RG (2011) Processes and impacts of Arctic amplification: a research synthesis. *Global and Planetary Change*, **77**, 85–96.

Serreze MC, Walsh JE, Chapin FS III *et al.* (2000) Observational evidence of recent change in the northern high-latitude environment. *Climatic Change*, **46**, 159–207.

Smith LC, Sheng Y, MacDonald GM, Hinzman LD (2005) Disappearing Arctic lakes. *Science*, **308**, 1429.

Stafford JM, Wendler G, Curtis J (2000) Temperature and precipitation of Alaska: 50 year trend analysis. *Theoretical and Applied Climatology*, **67**, 33–44.

Sturtevant CS, Oechel WC, Zona D, Kim Y, Emerson CE (2012) Soil moisture control over autumn season methane flux, Arctic Coastal Plain of Alaska. *Biogeosciences*, **9**, 1423–1440.

Takai K, Horikoshi K (2000) Rapid detection and quantification of members of the archaeal community by quantitative PCR using fluorogenic probes. *Applied and Environmental Microbiology*, **66**, 5066–5072.

Tokida T, Miyazaki T, Mizoguchi M, Nagata O, Takakai F, Kagemoto A, Hatano R (2007) Falling atmospheric pressure as a trigger for methane ebullition from peatland. *Global Biogeochemical Cycles*, **21**, GB2003.

Tscharntke T, Hochberg ME, Rand TA, Resh VH, Krauss J (2007) Author sequence and credit for contributions in multiauthored publications. *PLoS Biology*, **5**, e18.

Tsuyuzaki S, Nakano T, Kuniyoshi S, Fukuda M (2001) Methane flux in grassy marshlands near Kolyma River, north-eastern Siberia. *Soil Biology and Biochemistry*, **33**, 1419–1423.

Tveit AT, Urich T, Frenzel P, Svenning MM (2015) Metabolic and trophic interactions modulate methane production by Arctic peat microbiota in response to warming. *Proceedings of the National Academy of Sciences of the United States of America*, **112**, E2507–E2516.

Waddington JM, Day SM (2007) Methane emissions from a peatland following restoration. *Journal of Geophysical Research: Biogeosciences*, **112**, G03018.

Wagner D, Kobabe S, Pfeiffer E-MM, Hubberten H-WW (2003) Microbial controls on methane fluxes from a polygonal tundra of the Lena Delta, Siberia. *Permafrost and Periglacial Processes*, **14**, 173–185.

Walter KM, Zimov SA, Chanton JP, Verbyla D, Chapin FS (2006) Methane bubbling from Siberian thaw lakes as a positive feedback to climate warming. *Nature*, **443**, 71–75.

Westermann P (1993) Temperature regulation of methanogenesis in wetlands. *Chemosphere*, **26**, 321–328.

Whalen SC, Reeburgh WS (1992) Interannual variations in tundra methane emission: a 4-year time series at fixed sites. *Global Biogeochemical Cycles*, **6**, 139–159.

Whalen SC, Reeburgh WS (1996) Moisture and temperature sensitivity of CH_4 oxidation in boreal soils. *Soil Biology and Biochemistry*, **28**, 1271–1281.

Whitman WB, Bowen TL, Boone DR (2006) The methanogenic bacteria. In: *The Prokaryotes* (eds. Dworkin M, Falkow S, Rosenberg E, Schleifer K-H, Stackebrandt E), pp. 165–207. Springer, New York, NY.

Wille C, Kutzbach L, Sachs T, Wagner D, Pfeiffer EM (2008) Methane emission from Siberian arctic polygonal tundra: eddy covariance measurements and modeling. *Global Change Biology*, **14**, 1395–1408.

Yagi K, Tsuruta H, Kanda K, Minami K (1996) Effect of water management on methane emission from a Japanese rice paddy field: automated methane monitoring. *Global Biogeochemical Cycles*, **10**, 255–267.

Yimga MT, Dunfield PF, Ricke P, Heyer J, Liesack W (2003) Wide distribution of a novel pmoA-like gene copy among type II methanotrophs, and its expression in Methylocystis strain SC2. *Applied and Environmental Microbiology*, **69**, 5593–5602.

Yvon-Durocher G, Allen AP, Bastviken D *et al.* (2014) Methane fluxes show consistent temperature dependence across microbial to ecosystem scales. *Nature*, **507**, 488–491.

Zimov SA, Schuur EAG, Chapin FS (2006) Permafrost and the global carbon budget. *Science*, **312**, 1612–1613.

Zona D, Gioli B, Commane R *et al.* (2015) Cold season emissions dominate the Arctic tundra methane budget. *Proceedings of the National Academy of Sciences of the United States of America*, **113**, 40–45.

Supporting Information

Additional Supporting Information may be found in the online version of this article:

Table S1. The settings used for Covariance Matrix Adaptation Gene Expression Programming (CMAGEP) runs.
Table S2. Groups of methanogens found and substrates they use.
Table S3. Groups of methanotrophic bacteria, and enzymes that each genus possesses.
Figure S1. Diurnal variation in CH_4 flux rates along with soil and air temperatures.
Figure S2. Examples of CH_4 concentration ($[CH_4]$) change.
Figure S3. Gene copy numbers of archaea and bacteria by depth.